

O. NADTOKA, N. KUTSEVOL, T. BEZUGLA, P. VIRYCH, A. NAUMENKO

Taras Shevchenko National University of Kyiv

(64/13, Volodymyrs'ka Str., Kyiv 01601, Ukraine; e-mail: oksananadtoka@ukr.net)

## HYDROGEL-SILVER NANOPARTICLE COMPOSITES FOR BIOMEDICAL APPLICATIONS<sup>1</sup>

UDC 539

*Polyacrylamide and dextran-graft-polyacrylamide hydrogels are prepared and used as nanoreactors and networks for the synthesis of silver nanoparticles (AgNPs). Photochemical generation of AgNPs is carried out under UV-irradiation of Ag<sup>+</sup> ions in swollen hydrogels of different cross-linking densities. The obtained hydrogels and hydrogel/AgNPs composites are characterized by TEM, FTIR, and UV-Vis spectroscopy. Swelling studies have shown a relationship between the structure of the hydrogels and their ability to swell. It is shown that the presence of AgNPs in the polymer network leads to a decrease of the swelling capacity. An increase in the cross-linking density leads to an expansion of the AgNPs size distribution for both types of hydrogels. All synthesized hydrogel-silver nanoparticle composites have shown a high activity in the growth retardation of Staphylococcus aureus microorganisms.*

*Keywords:* silver nanoparticles, hydrogel, polyacrylamide, TEM, FTIR, UV-Vis spectroscopy.

### 1. Introduction

The inclusion of metal nanoparticles (NPs) in a polymer hydrogel network is a very attractive route for the development of nanocomposites for a wide range of applications. Hydrogels are known to be soft and elastic materials with high water retention. They are used in the production of biomaterials, artificial tissues, culture media, *etc.* [1]. The importance of metal nanoparticles follows from their magnetic, electronic, and optical performances. Being incorporated into a cross-linked polymer matrix, NPs essentially improve the mechanical properties of hydrogels [2]. They provide the nanocomposites with responsiveness to mechanical, thermal, magnetic, and electric stimuli, as well as to light [2, 3].

Commonly, the metal NPs in aqueous solutions are synthesized by reducing their salts. The dispersions of gold, silver, iron, copper, palladium, platinum, *etc.* NPs are fabricated from corresponding salt solutions in the presence of suitable chemical reductants, including glucose, hydrazine, ascorbic acid, sodium ascorbate, ethylene glycol, N-dimethylformamide, dextrose, sodium citrate, and sodium borohydride [4–7]. The biological use of NPs requires their hydrophilicity for a good dispersion in water. Hydrophilic polymers and surfactants are used to coat

nanoparticles, thus protecting NPs from the aggregation and agglomeration. Polyethylene oxide, polyacrylic and polymethacrylic acids, polyacrylamide, polyvinylpyrrolidone, polyvinyl alcohol, and some derivatives of macromolecular compounds of the natural origin are often used as stabilizing agents [8, 9]. In this case, steric stabilization can be achieved by the interaction of NPs with functional groups of polymer chains that prevent the aggregation through the steric repulsion.

Silver nanoparticles (AgNPs) are widely used in biotechnology and medicine. Three-dimensional polymer hydrogels loaded with AgNPs are considered to be materials with very high potential for medical therapeutic and diagnostic applications [10]. AgNPs can provide nanocomposites with antimicrobial activity, since they are able to bind non-specifically to bacterial membranes. Due to their own cytotoxicity, AgNPs are used as antibacterial and anticancer agents. The degree of toxicity against cells is determined by the surface charges of AgNPs [11]. AgNPs have plenty of unique multifunctionalities for biomedical applications, but the high instability and low biocompatibility still remain significant clinical challenges. The stabilization of nanoparticles in cross-

© O. NADTOKA, N. KUTSEVOL, T. BEZUGLA,  
P. VIRYCH, A. NAUMENKO, 2020

ISSN 0372-400X. Укр. фіз. журн. 2020. Т. 65, № 5

<sup>1</sup> The paper was presented at XXIVth Galyna Puchkovska International School-Seminar "Spectroscopy of Molecules and Crystals" (August 25–30, 2019, Odesa, Ukraine).

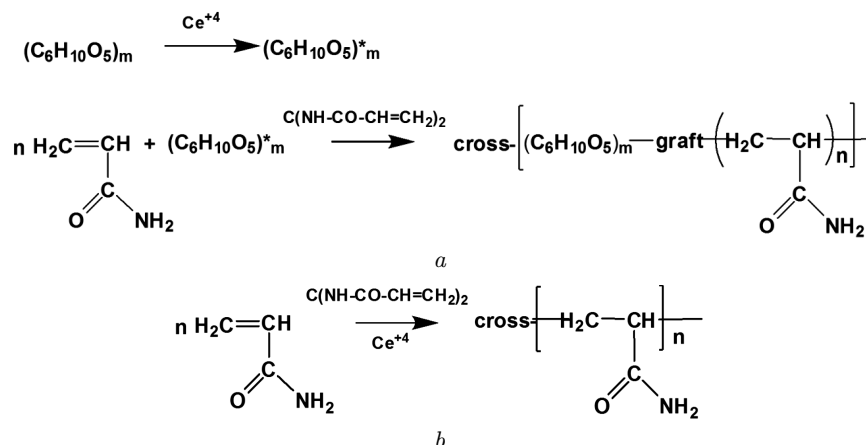


**Fig. 1.** Synthesis of hydrogels: cross-linked dextran-graft-polyacrylamide (a); cross-linked polyacrylamide (a)

linked hydrophilic polymers is an expected effect, when producing hydrogel/AgNPs composites. Therefore, the design and fabrication of novel biomaterials with desirable functions and excellent performances by the innovative combination of two completely different types of materials, namely hydrogels and metal NPs, attract great attention [12–15].

In fact, the porous structures of hydrogel networks are very suitable for the *in situ* formation of AgNPs, since the free space among the gel network provides a nanocontainer for the formation and growth of metal nanoparticles [12, 13].

This work is devoted to the comparative study of the cross-linked polyacrylamide- and dextran-graft-polyacrylamide-based hydrogels and their composites with AgNPs. We will focus on the effect of the hydrogel structure on the AgNPs formation and on properties of these nanosystems as materials for biomedical applications.

## 2. Experimental

### 2.1. Materials

#### 2.1.1. Chemicals

Acrylamide (AA) was supplied by Sigma, Germany. Dextran (D20) with  $M_w = 20000$  g/mol, cerium (IV) ammonium nitrate (CAN), N,N'-methylene-bis-acrylamide (MBA), silver nitrate (>99.9% pure) were purchased from Sigma-Aldrich. All supplied reagents were of the analytical grade and were used without further purification. Double deionized water was used throughout all procedures.

#### 2.1.2. Preparation of hydrogels

Dextran-graft-polyacrylamide (D20-g-PAA) hydrogels were prepared by the free radical polymerization, by using CAN as an initiator in the presence of cross-linking agent MBA [16] (Fig. 1, a). The calculated amount of dextran (0.02 mM) was dissolved in 25 mL of distilled water at 25 °C. This solution was purged by the argon bubbling for 20 min, and then initiator CAN (0.03 mM) was added. In 2 min, AA (0.05 mol) and MBA (0.2, 0.4, or 0.6 g per 100 g of monomer AA) were poured into the reaction mixture. The formed hydrogel samples were taken out from a flask in 24 h, washed with distilled water to remove the unreacted monomer. Finally, the gels were dried at ambient temperature. Polyacrylamide (PAA) hydrogels were prepared by the same procedure, but without the addition of dextran (Fig. 1, b).

The resulting hydrogels were designated as PAA- $x$  and D20-g-PAA- $x$ , where  $x = 0.2, 0.4$  or  $0.6$  according to the weight ratio of MBA to monomer AA (g/100 g) in the synthesis of the hydrogels. This value determines a cross-linking density in the hydrogel.

#### 2.1.3. Preparation of hydrogel/AgNPs composites

The dry hydrogels were placed in 0.1 M  $\text{AgNO}_3$  for 24 h for the swelling and saturation with  $\text{Ag}^+$  ions. Then hydrogels loaded with  $\text{Ag}^+$  ions were irradiated with UV light. Photochemical reactions were carried out under irradiation with a 1000-W medium-pressure mercury lamp for 5 min. The tube reactor was installed at a distance of 90 cm. Finally, the hydrogels with silver nanoparticles were dried

at ambient temperature. The samples were designated as PAAx/AgNPs and D20-g-PAA-*x*/AgNPs, respectively.

## 2.2. Methods

### 2.2.1. Swelling studies

The water absorption of dry hydrogels was studied gravimetrically. The dried samples were weighed, immersed in distilled water, and left to swell at 25 °C. Then they were taken out in certain periods of time, dried with thin filter paper, weighed on an analytical balance, and placed back into the same bath. The measurements were repeated until a constant weight of sample was achieved. The swelling ratio ( $S_t\%$ ) was calculated by the equation

$$S_t\% = \frac{m_\tau - m_0}{m_0} 100, \quad (1)$$

where  $m_t$  is the mass of hydrogel in the swollen state at time  $t$  and  $m_0$  is the mass of the dry hydrogel.

### 2.2.2. Characterization of hydrogel composites by FTIR-, UV-Vis spectroscopy, and scanning electron microscopy

A FTIR-spectrophotometer (MAGNA 550, Nicolet Instruments Corporation, USA) was used for the comparative characterization of pure hydrogel and hydrogel/AgNPs composite. We used the KBr technique for the sample preparation.

UV-visible spectra of hydrogel/AgNPs composites were recorded by using a Lambda 35 UV-Vis spectrophotometer (Perkin-Elmer, CA) in the absorbance mode (range 200–1000 nm). It was shown that this method is suitable for the characterization of nanosystems polymer/AgNPs [17]. All optical spectra were acquired, by using quartz cuvettes with 1-cm path length.

Scanning electron microscopy (SEM, Stereoscan 440; LEO, Cambridge, UK) was used to study the morphology of hydrogels. The samples of hydrogels were freeze-dried. The cryogenically fractured films in liquid nitrogen were mounted vertically on the SEM stub by a silver adhesive paste. The specimens were sputter coated with gold to avoid electrostatic charges and to improve the image resolution before being examined by the electron microscopy.

### 2.2.3. Microbiological tests

To test the materials for their ability to inhibit the bacterial growth, wild *Staphylococcus aureus* strains selectively obtained on Endo media and Yolk-salt agar were used. The sensitivity of the microorganisms was evaluated by the disc-diffusion method on a Müller–Hinton agar of the following composition (g/l): agar – 17, hydrolyzed casein – 17.5, hydrolyzed bovine hart – 2, starch – 1.5; pH = 7.3. The tested samples of the hydrogels and the composites were 5 mm in diameter, and their sizes were similar to those of standard disks with antibiotics. The control samples were PAA-*x*/AgNPs and D20-g-PAA-*x*/AgNPs hydrogels ( $x = 0.2, 0.4, \text{ or } 0.6$ ) saturated with 0.05% chlorhexidine solution.

Measurement of the growth retardation zone was performed, by using a digital caliper Miol 15–240. The contact of the studied hydrogel samples with microorganisms occurred within 24 h before the registration of the growth retardation diameter. The processing of statistical data was carried out by the Shapiro–Wilk test ( $p > 0.05$ ) and the Schaeff ANOVA test ( $p < 0.05$ ). Each experiment was repeated four times.

## 3. Results and Discussion

It was reported [18–19] that the structures of linear PAA and D20-g-PAA macromolecules are drastically different. D20-g-PAA is star-like polymer and its grafted PAA chains have a worm-like conformation in an aqueous solution. Being dissolved in water, molecules of linear PAA have a coil conformation. Obviously, cross-linked PAA and D20-g-PAA hydrogels should have different structures.

As shown by SEM images (Fig. 2), the morphologies of the PAA and D20-g-PAA hydrogels are different and essentially depend on the hydrogel composition.

Cross-linked PAA and D20-g-PAA hydrogels with various concentrations of cross-linking agent MBA were used both as nanoreactors for the synthesis of AgNPs and polymer networks for their stabilization. At the first stage of preparation of the nanocomposites, the hydrogel samples were saturated with an AgNO<sub>3</sub> solution. Silver ions have ability to interact with the functional moieties of a polymer network such as –OH, –NH<sub>2</sub>, –C=O groups [20]. At the next stage of synthesis, AgNPs were formed in free spaces

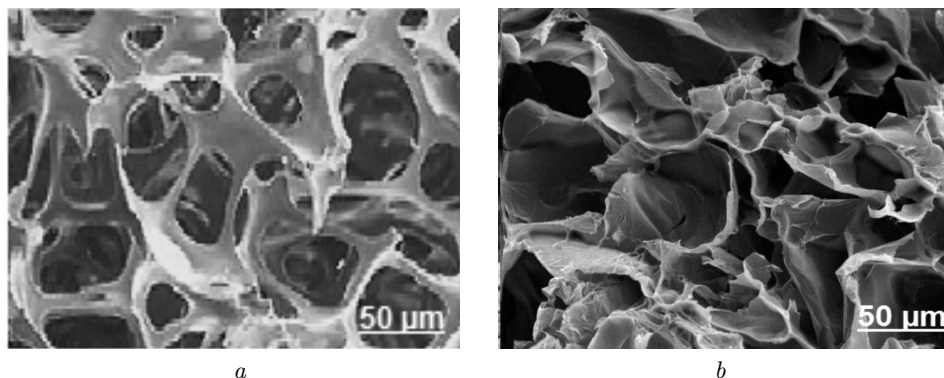


Fig. 2. SEM images of PAA (a) and D20-g-PAA (b) cross-linked hydrogels

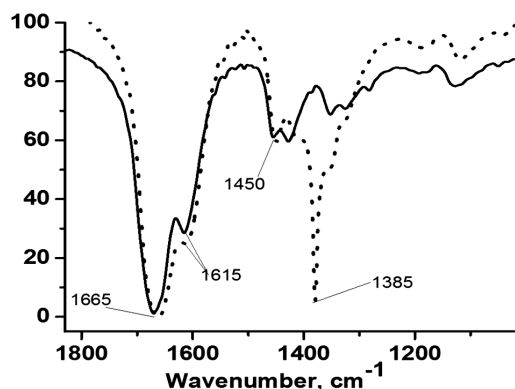


Fig. 3. Fragments of FTIR spectra: black – D20-g-PAA-0.4 hydrogel, red – D20-g-PAA-0.4/AgNPs composite

between the chains of the cross-linked polymeric network under UV-irradiation.

The FTIR spectra of the hydrogels and the hydrogel/AgNPs composites were recorded for all samples and demonstrated the same patterns.

As shown in Fig. 3, the characteristic peaks of the PAA component registered at  $1665\text{ cm}^{-1}$  ( $\nu(\text{C}=\text{O})$ , amide I) and  $1615\text{ cm}^{-1}$  ( $\delta(\text{N}-\text{H})$ , amide II) are observed both for D20-g-PAA-0.4 and D20-g-PAA-0.4/AgNPs samples. The peak at  $1450\text{ cm}^{-1}$  can be assigned to stretching vibrations in functional amide groups ( $\nu(\text{C}-\text{N})$ , amide III). The band at  $1385\text{ cm}^{-1}$  is typical of the IR spectra of the inorganic ion  $\text{NO}_3$ .

The  $\text{Ag}^+$ -loaded hydrogel is known to exhibit a significant shift in the amide peak, i.e.,  $1654\text{ cm}^{-1}$ , due to the complexation of silver ions with amide groups [21]. However, for our systems, this effect is not observed. Thus, silver predominantly exists as sil-

ver nanoparticles and only the negligible amount of  $\text{Ag}^+$  ions can be present in swollen hydrogels.

The absorption spectra for two types of samples, PAA- $x$  and D20-g-PAA- $x$  hydrogels with incorporated AgNPs, were analyzed in the UV-visible region (Fig. 4).

It is widely known that the adsorption peak at 298 nm can be registered for an  $\text{AgNO}_3$  solution and corresponds to  $\text{Ag}^+$  ions [21]. The procedure of hydrogel/AgNPs preparation assumes the presence of residual  $\text{Ag}^+$  ions in the swollen cross-linked polymer (Fig. 4).

The peak registered in the range 380–850 nm can be attributed to the surface plasmon resonance (SPR) band. It is known that the composition, size, and shape of nanoparticles can affect the collective oscillations of free electrons in metallic NPs at their SPR wavelengths, when irradiated with resonant light [22]. The width of the SPR band is related to the size distribution of AgNPs.

As shown in Fig. 4, a, the UV-Vis spectra of PAA- $x$ /AgNPs samples have wide SPR band, thus indicating a rather wide particle size distribution in these composites. The changes in the cross-linking density lead to changes in the shape and width of the SPR band. The spectra of PAA- $x$ /AgNPs composites demonstrate the appearance of a shoulder on the absorption curve in the long wavelength region, which increases with  $x$  (ratio of the cross-linking agent MBA to monomer AA). The same effect of the SPR band broadening with increasing  $x$  is registered for D20-g-PAA- $x$ /AgNPs composites, but the long wavelength shoulder is less pronounced (Fig. 4, b). All parameters of the SPR band are determined by the shape

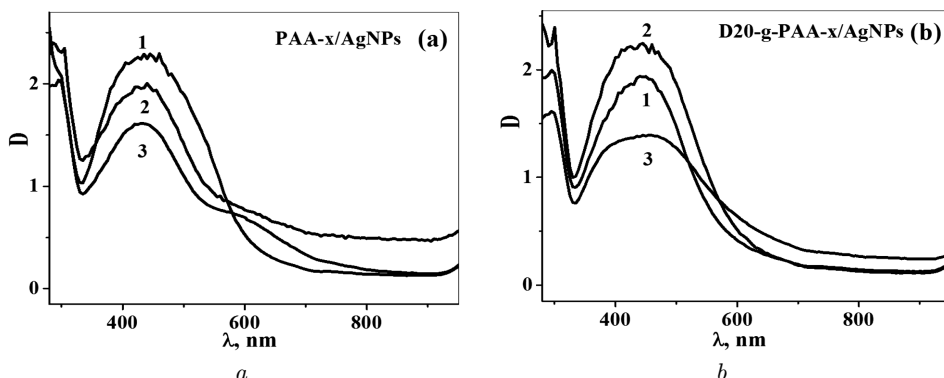


Fig. 4. UV-Vis adsorption spectra of PAA- $x$ /AgNPs (a) and D20-g-PAA- $x$ /AgNPs (b) composites with different cross-linking densities ( $x = 0.2$  (1); 0.4 (2); 0.6 (3))

and size distributions of nanoparticles, the formation of which is determined by the structural features of cross-linked polymer matrices. Thus, the structure of D20-g-PAA-0.2 hydrogel is optimal for obtaining an AgNPs-loaded composite with a narrower particle size distribution.

Thus, the morphology of the hydrogel affects the process of AgNPs formation and, therefore, should determine important properties of the hydrogel nanocomposites as materials for biomedical application.

All synthesized hydrogels, as well as AgNPs-loaded composites, were tested for their swelling capacity (Table).

The values of the swelling ability in the equilibrium state ( $S_{eq}$ ) for cross-linked D20-g-PAA samples are higher than those for cross-linked PAA at the same concentrations of the cross-linking agent MBA. This can be explained by the different mesh structures of hydrogels. It can be seen that the pores in the hydrogels based on D20-g-PAA have lake-like shape (Fig. 2). An increase in the MBA concentration leads to a decrease in the swelling capacity for both series of samples, which indicates the formation of a hydrogel network with a higher density.

The data in Table demonstrate the difference in the swelling capacities of synthesized nanocomposites based of PAA and D20-g-PAA hydrogels. The PAA- $x$ /AgNPs and D20-g-PAA- $x$ /AgNPs samples demonstrate lower values of the swelling capacity (Table) compared to their hydrogel analogs without silver nanoparticles. As an example, the effect of AgNPs incorporated into PAA-0.4 and D20-g-PAA-0.4 hydrogels on their swelling behaviors is shown in Fig. 5. It is evident that hydrogels loaded with Ag-

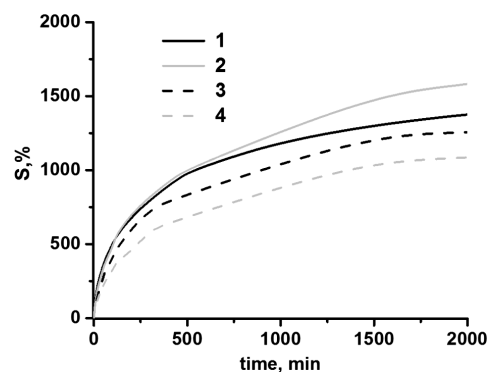


Fig. 5. Swelling behavior of hydrogels and hydrogel/AgNPs composites: PAA-0.4 (1), D20-g-PAA-0.4 (2), PAA-0.4/AgNPs (3), and D20-g-PAA-0.4/AgNPs (4)

#### Swelling capacity of hydrogels and hydrogel/AgNPs composites

Hydrogel	$x^*$	$S_{eq}^{**}$ , % (without AgNPs)	$S_{eq}^{**}$ , % (with AgNPs)
Cross-linked PAA	0.2	1530	1330
Cross-linked PAA	0.4	1400	1250
Cross-linked PAA	0.6	1340	1200
Cross-linked D20-g-PAA	0.2	1980	1270
Cross-linked D20-g-PAA	0.4	1580	1060
Cross-linked D20-g-PAA	0.6	1370	990

\* The weight ratio of MBA to monomer AA (g/100 g) in the synthesis of the hydrogels.

\*\* The error limit is  $\pm 10\%$  (no less than 5 swelling experiments).

NPs have lower swelling ratios than corresponding pure hydrogels. This regularity is inherent in all PAA- $x$ /AgNPs and D20-g-PAA- $x$ /AgNPs samples. It can be explained by additional cross-links between Ag-

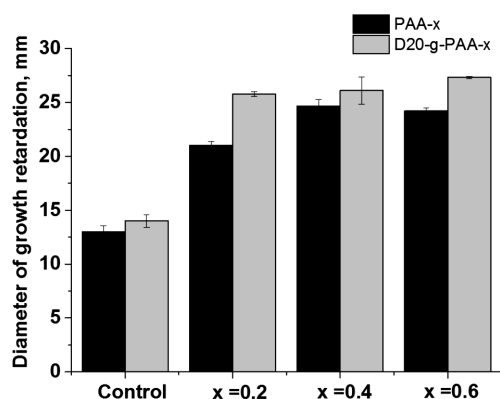


**Fig. 6.** Diameter of the growth retardation of *Staphylococcus aureus* after the use of PAA- $x$  and D20-g-PAA- $x$  hydrogels loaded with chlorhexidine (Control) and AgNPs ( $x = 0.2, 0.4$ , or  $0.6$ )

NPs and functional groups of polymer side-chains, which lead to a decrease in the permeability of hydrogel composites to water and a change in the overall swelling characteristic [8]. The interaction of AgNPs with the side chains of the polymer increases the rigidity of the hydrogel network and reduces its hydrophilicity. Both of these processes lead to a decrease in the ability of hydrogels to swell.

Microbiological tests of PAA- $x$  and D20-g-PAA- $x$  samples loaded with chlorhexidine demonstrated almost the same growth retardation of *Staphylococcus aureus* microorganisms. The growth retardation diameters were 13–15 mm, and these values did not depend on the ratio of crosslinking agent MBA to AA monomer in hydrogels. There are control samples in Fig. 6 which demonstrate the growth retardation of *Staphylococcus aureus* after the use of hydrogels loaded with chlorhexidine.

It is evident that the hydrogels loaded with silver nanoparticles are much more active in the growth inhibition of *Staphylococcus aureus* (Fig. 6). The growth retardation diameters are essentially larger than those of chlorhexidine-loaded samples and reach 21–27 mm. For all hydrogel/AgNPs-composites, a visible excess of these values for D20-g-PAA- $x$ /AgNPs samples compared to the corresponding PAA- $x$ /AgNPs ones is observed. A trend of the activity of composites increasing with the degree of crosslinking was registered. Thus, the peculiarities of the internal structure of hydrogels should be taken into account in manufacturing the AgNPs-loaded materials.

#### 4. Conclusions

Polyacrylamide and dextran-graft-polyacrylamide hydrogels with different cross-linking densities are synthesized by the radical polymerization. The hydrogel samples are used as nanoreactors for the generation of silver nanoparticles by the photochemical reduction of  $\text{AgNO}_3$  under UV-irradiation. The structure of hydrogels and their cross-linking density appear to be the key factors for the *in situ* formation of AgNPs in hydrogels. The presence of AgNPs in a polymer network leads to decreasing the swelling ability. The FTIR spectra of hydrogels and hydrogel/AgNPs composites are very close, indicating an almost complete conversion of silver ions to silver nanoparticles. The significant SPR band width in the UV-Vis spectra of all AgNPs-loaded composites is associated with a wide size distribution of AgNPs which expands with an increase of the cross-linking densities of hydrogels. According to microbiological studies, the obtained composites are active in the growth retardation of microorganisms and can be used in a wide range of biomedical applications.

1. K. Pal, A.K. Bantia, D.K. Majumdar. Polymeric hydrogel: Characterization and biomedical applications. *Design. Monom. Polym.* **12** (3), 197 (2009).
2. M. Biondi, A. Borzacchiello, L. Mayol, L. Ambrosio. Nanoparticle-integrated hydrogels as multifunctional composite materials for biomedical applications. *Gels* **1**, 162 (2015).
3. J. Bai, Y. Li, J. Du, S. Wang, J. Zheng, Q. Yang, X. Chen. One-pot synthesis of polyacrylamide-gold nanocomposite. *Mater. Chem. Phys.* **106**, 412 (2007).
4. C. Kinnear, T.L. Moore, L. Rodriguez-Lorenzo, B. Rothen-Rutishauser, A. Petri-Fink. Form follows function: Nanoparticle shape and its implications for nanomedicine. *Chem. Rev.* **117**, 11476 (2017).
5. P.J.G. Goulet, R.B. Lennox. New insights into Brust-Schiffrin metal nanoparticle synthesis. *J. Am. Chem. Soc.* **132**, 9582 (2010).
6. D.D. Evanoff, G. Chumanov. Synthesis and optical properties of silver nanoparticles and arrays. *Chem. Phys. Chem.* **6**, 1221 (2005).
7. X.-F. Zhang, Zh.-G. Liu, W. Shen, S. Gurunathan. Silver nanoparticles: synthesis, characterization, properties, applications, and therapeutic approaches. *Int. J. Mol. Sci.* **17**, 1534 (2016).
8. S. Agnihotri, S. Mukherji, S. Mukherji. Antimicrobial chitosan-PVA hydrogel as a nanoreactor and immobilizing matrix for silver nanoparticles. *Appl. Nanosci.* **2** (3), 179 (2012).

9. Z.S. Pillai, P.V. Kamat. What factors control the size and shape of silver nanoparticles in the citrate ion reduction method? *J. Phys. Chem. B* **108**, 945 (2004).
10. A.K. Suresh, D.A. Pelletier, W. Wang, J.L. Morrell-Falvey, B.Gu, M.J. Doktycz. Cytotoxicity induced by engineered silver nanocrystallites is dependent on surface coatings and cell types. *Langmuir* **28**, 2727 (2012).
11. P. Schlunkert, E. Casals, M. Boyles, U. Tischler, E. Hornig, N. Tran, J. Zhao, M. Himly, M. Riediker, G.J. Oostingh, et al. The oxidative potential of differently charged silver and gold nanoparticles on three human lung epithelial cell types. *J. Nanobiotechnol.* **13**, 1 (2015).
12. P. Thoniyot, M.J. Tan, A.A. Karim, D.J. Young, X.J. Loh, Nanoparticle-hydrogel composites: Concept, design and applications of these promising, multi-functional materials. *Adv. Sci.* **2** (1–2), 1400010 (2015).
13. V. Thomas, M. Namdeo, Y.M. Mohan, S.K. Bajpai, M. Bajpai, Review on polymer, hydrogel and microgel metal nanocomposites: A facile nanotechnological approach. *J. Macromol. Sci. Pure Appl. Chem.* **45**, 107 (2008).
14. A.K. Gaharwar, N.A. Peppas, A. Khademhosseini. Nanocomposite hydrogels for biomedical applications. *Biotechnol. Bioeng.* **111**, 441 (2014).
15. S. Xu, L. Deng, J. Zhang, L. Yin, A. Dong. Composites of electrospun-fibers and hydrogels: A potential solution to current challenges in biological and biomedical field. *J. Biomed. Mater. Res. B* **104** (3), 640 (2015).
16. O. Nadtoka, N. Kutsevol, V. Krysa, B. Krysa. Hybrid polyacryamide hydrogels: Synthesis, properties and prospects of application. *Mol. Cryst. Liq. Cryst.* **672** (1), 1 (2018).
17. L. Bulavin, N. Kutsevol, V. Chumachenko, D. Soloviov, A. Kuklin, A. Marinin. SAXS combined with UV-vis spectroscopy and QUELS: accurate characterization of silver sols synthesized in polymer matrices. *Nanoscale Res. Lett.* **11**, 35 (2016).
18. N. Kutsevol, J.M. Guenet, N. Melnyk, D. Sarazin, C. Rochas. Solution properties of dextran-polyacrylamide graft copolymers. *Polymer* **47**, 2061 (2006).
19. M. Bezuglyi, N. Kutsevol, M. Rawiso, T. Bezugla. Water-soluble branched copolymers dextran-polyacrylamide and their anionic derivatives as matrices for metal nanoparticles *in-situ* synthesis. *Chemik* **8** (66), 862 (2012).
20. P. Murthy, Y. Murali Mohan, K. Varaprasad, B. Sreedhar, K. Mohana Raju. First successful design of semi-IPN hydrogel-silver nanocomposites: a facile approach for antibacterial application. *J. Colloid. Interface Sci.* **318** (2), 217 (2008).
21. K. Varaprasad, Y. Murali Mohan, S. Ravindra, N. Narayana Reddy, K. Vimala, K. Monika, B. Sreedhar, K. Mohana Raju. Hydrogel-silver nanoparticle composites: a new generation of antimicrobials. *J. App. Polymer Sci.* **115**, 1199 (2010).
22. S.H. Lee, B.-H. Jun. Silver nanoparticles: synthesis and application for nanomedicine. *Int. J. Mol. Sci.* **20** (4), 865 (2019).

Received 13.01.20

*О. Надтока, Н. Куцевол,  
Т. Безугла, П. Вірич, А. Науменко*

#### ГІДРОГЕЛІВІ КОМПОЗИТИ З НАНОЧАСТИНКАМИ СРІБЛА ДЛЯ БІОМЕДИЧНОГО ЗАСТОСУВАННЯ

#### Резюме

Синтезовано гідрогелі на основі поліакриламіді та прищеплених кополімерів декстран-поліакриламіді та використано їх як нанореактори для синтезу наночастинок срібла (AgNPs). Фотохімічну генерацію AgNP проводили при УФ-опроміненні іонів Ag<sup>+</sup> у насичених розчиніом гідрогелях із різним ступенем зшивання. Отримані гідрогелі та композити гідрогель/AgNPs характеризувались за допомогою ТЕМ та спектроскопії в інфрачервоному, видимому та ультрафіолетовому діапазонах спектра. Дослідження набухання показали залежність між будовою гідрогелів та їх здатністю до набухання. Було показано, що наявність AgNP у полімерній сітці призводить до зниження здатності до набухання. Збільшення ступеня зшивання приводить до розширення розподілу розмірів AgNP для обох типів гідрогелів. Усі синтезовані композити гідрогель/AgNPs виявили високу активність у інгібуванні росту мікроорганізмів *Staphylococcus aureus*.